

Velocity and Temperature Distributions Between Parallel Porous Plates with the Hall Effect and Variable Properties Under Exponential Decaying Pressure Gradient

Hazem Ali ATTIA¹⁾, Mostafa A.M. ABDEEN²⁾

¹⁾ *Fayoum University, Faculty of Engineering
Department of Engineering Mathematics and Physics
El-Fayoum-63514, Egypt
e-mail: ah1113@yahoo.com*

²⁾ *Cairo University, Faculty of Engineering
Department of Engineering Mathematics and Physics
Giza 12211, Egypt
e-mail: mostafa_a_m_abdeen@hotmail.com*

The time varying hydromagnetic flow between two infinite parallel porous plates is studied with heat transfer considering the Hall effect and temperature dependent physical properties. An exponential decaying pressure gradient is imposed in the axial direction and an external uniform magnetic field as well as a uniform suction and injection are applied perpendicular to the horizontal plates. A numerical solution for the governing non-linear coupled set of equations of motion and the energy equation is adopted. The effects of the Hall current and the temperature dependent viscosity and thermal conductivity on both the velocity and temperature distributions are investigated.

Key words: flow between parallel plates, variable properties, hydromagnetics, heat transfer, numerical solution.

1. INTRODUCTION

The flow of an electrically conducting fluid between infinite horizontal parallel plates, known as Hartmann flow, has interesting applications in magnetohydrodynamic (MHD) power generators and pumps etc. HARTMANN and LAZARUS [1] investigated the effect of a transverse uniform magnetic field on the flow of a viscous incompressible electrically conducting fluid between two infinite parallel plates. Exact solutions for the velocity fields were developed [2–5] under different physical effects. Some exact and numerical solutions for the heat transfer problem are derived in [6]. SOUNDALGEKAR *et al.* [7, 8] examined the

effect of Hall currents on the steady MHD Couette flow with heat transfer. The temperatures of the two plates were assumed constant [7] or varying along the plates in the direction of the flow [8]. ATTIA [9] examined the effect of Hall current on the velocity and temperature fields of an unsteady Hartmann flow with uniform suction and injection applied perpendicular to the plates.

In these studies the physical properties are assumed to be constant, however it is known that some physical properties are functions of temperature and assuming constant properties is a good approximation as long as small differences in temperature are involved. More accurate prediction for the flow and heat transfer can be achieved by considering the variation of the physical properties with temperature [10]. KLEMP *et al.* [11] studied the effect of temperature dependent viscosity on the entrance flow in a channel in the hydrodynamic case. ATTIA and KOTB [12] solved the steady MHD fully developed flow and heat transfer between two parallel plates with temperature dependent viscosity which has been extended to the transient state by ATTIA [13]. The influence of the dependence of the physical properties on temperature in the MHD Couette flow between parallel plates was studied [14, 15].

In this work, the unsteady Hartmann flow of a viscous incompressible electrically conducting fluid is investigated with heat transfer. The viscosity and thermal conductivity of the fluid are assumed to vary with temperature and the Hall current is considered. The fluid is flowing between two electrically insulating porous plates and is acted upon by an exponential decaying pressure gradient. A uniform suction and injection and an external uniform magnetic field are applied normal the surface of the plates. The two plates are kept at two constant but different temperatures and the viscous and Joule dissipations terms are included in the energy equation. This configuration is a good approximation of some practical situations such as heat exchangers, flow meters, and pipes that connect system components. The flow and temperature distributions of both the fluid and dust particles are governed by the coupled set of the momentum and energy equations. The coupled set of non-linear equations of motion and the energy equation are solved numerically using finite differences to determine the velocity and temperature fields.

2. FORMULATION OF THE PROBLEM

The fluid flow is between two infinite horizontal parallel plates located at the $y = \pm h$ planes. The two plates are porous, insulating and kept at two constant but different temperatures T_1 for the lower plate and T_2 for the upper one with $T_2 > T_1$. An exponential decaying pressure gradient is imposed in the axial x -direction and a uniform suction from above and injection from below, with velocity v_0 , are applied impulsively at $t = 0$. A uniform magnetic field B_0 ,

assumed unaltered, is applied perpendicular to the plates in the positive y -direction. The Hall effect is considered and accordingly, a z -component of the velocity is initiated. The viscosity and thermal conductivity of the fluid depend on temperature exponentially and linearly, respectively while the viscous and Joule dissipations are not neglected in the energy equation. The fluid motion starts from rest at $t = 0$, and the no-slip condition at the plates implies that the fluid velocity has neither a z - nor an x -component at $y = \pm h$. The initial temperature of the fluid is assumed to be equal to T_1 as the temperature of the lower plate. Since the plates are infinite in the x - and z -directions, the physical quantities do not change in these directions which leads to one-dimensional problem.

The flow of the fluid is governed by the Navier–Stokes equation

$$(2.1) \quad \rho \frac{D\mathbf{v}}{Dt} = -\nabla p + \nabla \cdot (\mu \nabla \mathbf{v}) + \mathbf{J} \wedge \mathbf{B}_0,$$

where ρ is the density of the fluid, μ is the viscosity of the fluid, \mathbf{J} is the current density, and \mathbf{v} is the velocity vector of the fluid, which is given by

$$\mathbf{v} = u(y, t)\mathbf{i} + v_0\mathbf{j} + w(y, t)\mathbf{k}.$$

If the Hall term is retained, the current density \mathbf{J} is given by the generalized Ohm's law [4]

$$(2.2) \quad \mathbf{J} = \sigma(\mathbf{v} \wedge \mathbf{B}_0 - \beta(\mathbf{J} \wedge \mathbf{B}_0)),$$

where σ is the electric conductivity of the fluid and β is the Hall factor [4]. Equation (2.2) may be solved in \mathbf{J} to yield

$$(2.3) \quad \mathbf{J} \wedge \mathbf{B}_0 = -\frac{\sigma B_0^2}{1+m^2}((u+mw)\mathbf{i} + (w-mu)\mathbf{k}),$$

where m is the Hall parameter and $m = \sigma\beta B_0$. Thus, the two components of the momentum equation (2.1) read

$$(2.4) \quad \rho \frac{\partial u}{\partial t} + \rho v_0 \frac{\partial u}{\partial y} = Ge^{-\alpha t} + \mu \frac{\partial^2 u}{\partial y^2} + \frac{\partial \mu}{\partial y} \frac{\partial u}{\partial y} - \frac{\sigma B_0^2}{1+m^2}(u+mw),$$

$$(2.5) \quad \rho \frac{\partial w}{\partial t} + \rho v_0 \frac{\partial w}{\partial y} = \mu \frac{\partial^2 w}{\partial y^2} + \frac{\partial \mu}{\partial y} \frac{\partial w}{\partial y} - \frac{\sigma B_0^2}{1+m^2}(w-mu).$$

It is assumed that the pressure gradient is applied at $t = 0$ and the fluid starts its motion from rest. Thus

$$(2.6)_1 \quad t = 0: u = w = 0.$$

For $t > 0$, the no-slip condition at the plates implies that

$$(2.6)_2 \quad y = -h: u = w = 0,$$

$$(2.6)_3 \quad y = h: u = w = 0.$$

The energy equation describing the temperature distribution for the fluid is given by [15]

$$(2.7) \quad \rho c_p \frac{\partial T}{\partial t} + \rho c_p v_0 \frac{\partial T}{\partial y} = \frac{\partial}{\partial y} \left(k \frac{\partial T}{\partial y} \right) + \mu \left[\left(\frac{\partial u}{\partial y} \right)^2 + \left(\frac{\partial w}{\partial y} \right)^2 \right] + \frac{\sigma B_0^2}{1 + m^2} (u^2 + w^2),$$

where T is the temperature of the fluid, c_p is the specific heat at constant pressure of the fluid, and k is thermal conductivity of the fluid. The last two terms in the right side of Eq. (2.7) represent the viscous and Joule dissipations respectively.

The temperature of the fluid must satisfy the initial and boundary conditions,

$$(2.8) \quad \begin{aligned} t = 0: T &= T_1, \\ t > 0: T &= T_1, \quad y = -h, \\ t > 0: T &= T_2, \quad y = h. \end{aligned}$$

The viscosity of the fluid is assumed to vary with temperature and is defined as, $\mu = \mu_0 f_1(T)$. By assuming the viscosity to vary exponentially with temperature, the function $f_1(T)$ takes the form [7], $f_1(T) = \exp(-a_1(T - T_1))$. In some cases a_1 may be negative, i.e. the coefficient of viscosity increases with temperature [7, 15]. Also the thermal conductivity of the fluid is varying with temperature as $k = k_0 f_2(T)$. We assume linear dependence for the thermal conductivity upon the temperature in the form $k = k_0[1 + b_1(T - T_1)]$ [16], where the parameter b_1 may be positive or negative [16].

Introducing the following non-dimensional quantities,

$$\begin{aligned} (\hat{x}, \hat{y}, \hat{z}) &= \frac{(x, y, z)}{h}, & \hat{t} &= \frac{t \mu_0}{\rho h^2}, \\ \hat{G} &= \frac{\rho G}{h^2 \mu_0^2}, & (\hat{u}, \hat{w}) &= \frac{(u, w) \rho h}{\mu_0}, \\ \theta &= \frac{T - T_1}{T_2 - T_1}, \end{aligned}$$

where

$$\widehat{f}_1(\theta) = e^{-a_1(T_2-T_1)\theta} = e^{-a\theta}, \quad a \text{ is the viscosity variation parameter,}$$

$$\widehat{f}_2(\theta) = 1 + b_1(T_2 - T_1)\theta = 1 + b\theta, \quad b \text{ is the thermal conductivity variation parameter,}$$

$$S = \rho v_0 h / \mu_0 \text{ is the suction parameter,}$$

$$\text{Ha}^2 = \sigma B_0^2 h^2 / \mu_0, \text{ Ha is the Hartmann number,}$$

$$\text{Pr} = \mu_0 c_p / k_0 \text{ is the Prandtl number,}$$

$$\text{Ec} = \mu_0^2 / h^2 c_p \rho^2 (T_2 - T_1) \text{ is the Eckert number.}$$

Equations (2.4) to (2.8) read (the hats are dropped for simplicity)

$$(2.9) \quad \frac{\partial u}{\partial t} + S \frac{\partial u}{\partial y} = Ge^{-\alpha t} + f_1(\theta) \frac{\partial^2 u}{\partial y^2} + \frac{\partial f_1(\theta)}{\partial y} \frac{\partial u}{\partial y} - \frac{\text{Ha}^2}{1+m^2}(u+mw),$$

$$(2.10) \quad \frac{\partial w}{\partial t} + S \frac{\partial w}{\partial y} = f_1(\theta) \frac{\partial^2 w}{\partial y^2} + \frac{\partial f_1(\theta)}{\partial y} \frac{\partial w}{\partial y} - \frac{\text{Ha}^2}{1+m^2}(w-mu),$$

$$t = 0: \quad u = w = 0,$$

$$(2.11) \quad t > 0: \quad y = -1, \quad u = w = 0,$$

$$t > 0: \quad y = 1, \quad u = w = 0,$$

$$(2.12) \quad \frac{\partial \theta}{\partial t} + S \frac{\partial \theta}{\partial y} = \frac{1}{\text{Pr}} f_2(\theta) \frac{\partial^2 \theta}{\partial y^2} + \frac{1}{\text{Pr}} \frac{\partial f_2(\theta)}{\partial y} \frac{\partial \theta}{\partial y} \\ + \text{Ec} f_1(\theta) \left[\left(\frac{\partial u}{\partial y} \right)^2 + \left(\frac{\partial w}{\partial y} \right)^2 \right] + \frac{\text{Ec} \text{Ha}^2}{1+m^2}(u^2+w^2),$$

$$t = 0: \quad \theta = 0,$$

$$(2.13) \quad t > 0: \quad \theta = 0, \quad y = -1,$$

$$t > 0: \quad \theta = 1, \quad y = 1.$$

Equations (2.9), (2.10), and (2.12) represent a system of coupled non-linear partial differential equations which are solved numerically under the initial and boundary conditions (2.11) and (2.13) using the method of finite differences. A linearization technique is first applied to replace the nonlinear terms at a linear stage, with the corrections incorporated in subsequent iterative steps until convergence is reached. Then the Crank–Nicolson implicit method is used at two successive time levels [17]. An iterative scheme is used to solve the linearized system of difference equations. The solution at a certain time step is chosen as an initial guess for next time step and the iterations are continued till convergence,

within a prescribed accuracy. Finally, the resulting block tridiagonal system is solved using the generalized Thomas-algorithm [17]. Finite difference equations relating the variables are obtained by writing the equations at the mid point of the computational cell and then replacing the different terms by their second order central difference approximations in the y -direction. The diffusion terms are replaced by the average of the central differences at two successive time-levels. The computational domain is divided into meshes each of dimension Δt and Δy in time and space, respectively. We define the variables $A = \partial u / \partial y$, $B = \partial w / \partial y$ and $H = \partial \theta / \partial y$ to reduce the second order differential equations (2.9), (2.10) and (2.12) to first-order differential equations which take the form

$$\begin{aligned}
 (2.14) \quad & \left(\frac{u_{i+1,j+1} - u_{i,j+1} + u_{i+1,j} - u_{i,j}}{2} \right) + S \left(\frac{A_{i+1,j+1} + A_{i,j+1} + A_{i+1,j} + A_{i,j}}{4} \right) \\
 & = G \exp \left[-\alpha \left(\frac{t_{i+1} + t_i}{2} \right) \right] + \left(\frac{\bar{f}_1(\theta)_{i,j+1} + \bar{f}_1(\theta)_{i,j}}{2} \right) \\
 & \cdot \left(\frac{(A_{i+1,j+1} + A_{i,j+1}) - (A_{i+1,j} + A_{i,j})}{2\Delta y} \right) + \left(\frac{\bar{f}_1(\theta)_{i,j+1} - \bar{f}_1(\theta)_{i,j}}{\Delta y} \right) \\
 & \cdot \left(\frac{A_{i+1,j+1} + A_{i,j+1} + A_{i+1,j} + A_{i,j}}{4} \right) \\
 & - \frac{\text{Ha}^2}{1+m^2} \left(\frac{u_{i+1,j+1} + u_{i,j+1} + u_{i+1,j} + u_{i,j}}{4} \right) \\
 & - \frac{m\text{Ha}^2}{1+m^2} \left(\frac{w_{i+1,j+1} + w_{i,j+1} + w_{i+1,j} + w_{i,j}}{4} \right),
 \end{aligned}$$

$$\begin{aligned}
 (2.15) \quad & \left(\frac{w_{i+1,j+1} - w_{i,j+1} + w_{i+1,j} - w_{i,j}}{2} \right) + S \left(\frac{B_{i+1,j+1} + B_{i,j+1} + B_{i+1,j} + B_{i,j}}{4} \right) \\
 & = \left(\frac{\bar{f}_1(\theta)_{i,j+1} + \bar{f}_1(\theta)_{i,j}}{2} \right) \left(\frac{(B_{i+1,j+1} + B_{i,j+1}) - (B_{i+1,j} + B_{i,j})}{2\Delta y} \right) \\
 & + \left(\frac{\bar{f}_1(\theta)_{i,j+1} - \bar{f}_1(\theta)_{i,j}}{\Delta y} \right) \left(\frac{B_{i+1,j+1} + B_{i,j+1} + B_{i+1,j} + B_{i,j}}{4} \right) \\
 & - \frac{\text{Ha}^2}{1+m^2} \left(\frac{w_{i+1,j+1} + w_{i,j+1} + w_{i+1,j} + w_{i,j}}{4} \right) \\
 & + \frac{m\text{Ha}^2}{1+m^2} \left(\frac{u_{i+1,j+1} + u_{i,j+1} + u_{i+1,j} + u_{i,j}}{4} \right),
 \end{aligned}$$

$$\begin{aligned}
(2.16) \quad & \left(\frac{\theta_{i+1,j+1} - \theta_{i,j+1} + \theta_{i+1,j} - \theta_{i,j}}{2\Delta t} \right) + S \left(\frac{H_{i+1,j+1} + H_{i,j+1} + H_{i+1,j} + H_{i,j}}{4} \right) \\
& = \left(\frac{\bar{f}_2(\theta)_{i,j+1} + \bar{f}_2(\theta)_{i,j}}{2\text{Pr}} \right) \left(\frac{(H_{i+1,j+1} + H_{i,j+1}) - (H_{i+1,j} + H_{i,j})}{2\Delta y} \right) \\
& \quad + \left(\frac{\bar{f}_2(\theta)_{i,j+1} - \bar{f}_2(\theta)_{i,j}}{\Delta y} \right) \left(\frac{H_{i+1,j+1} + H_{i,j+1} + H_{i+1,j} + H_{i,j}}{4\text{Pr}} \right) \\
& - \text{Ec} \left(\frac{\bar{f}_1(\theta)_{i,j+1} + \bar{f}_1(\theta)_{i,j}}{2} \right) \left(\frac{(\bar{A}_{i+1,j+1} + \bar{A}_{i,j+1} + \bar{A}_{i+1,j} + \bar{A}_{i,j})}{2} \right) \\
& \quad \cdot \left(\frac{A_{i+1,j+1} + A_{i,j+1} + A_{i+1,j} + A_{i,j}}{2} \right) \\
& + \text{Ec} \left(\frac{\bar{f}_1(\theta)_{i,j+1} + \bar{f}_1(\theta)_{i,j}}{2} \right) \left(\frac{(\bar{B}_{i+1,j+1} + \bar{B}_{i,j+1} + \bar{B}_{i+1,j} + \bar{B}_{i,j})}{2} \right) \\
& \quad \cdot \left(\frac{B_{i+1,j+1} + B_{i,j+1} + B_{i+1,j} + B_{i,j}}{2} \right) \\
& \quad + \frac{\text{Ec Ha}^2}{1+m^2} \left(\frac{\bar{u}_{i+1,j+1} + \bar{u}_{i,j+1} + \bar{u}_{i+1,j} + \bar{u}_{i,j}}{2} \right) \\
& \quad \cdot \left(\frac{u_{i+1,j+1} + u_{i,j+1} + u_{i+1,j} + u_{i,j}}{2} \right) \\
& \quad + \frac{\text{Ec Ha}^2}{1+m^2} \left(\frac{\bar{w}_{i+1,j+1} + \bar{w}_{i,j+1} + \bar{w}_{i+1,j} + \bar{w}_{i,j}}{2} \right) \\
& \quad \cdot \left(\frac{w_{i+1,j+1} + w_{i,j+1} + w_{i+1,j} + w_{i,j}}{2} \right).
\end{aligned}$$

The variables with bars are given initial guesses from the previous time steps and an iterative scheme is used at every time to solve the linearized system of difference equations. All calculations have been carried out for the non-dimensional variables and parameters given by: $G = 5$, $\alpha = 1$, $\text{Pr} = 1$, and $\text{Ec} = 0.2$. Grid-independence studies show that the computational domain $0 < t < \infty$ and $-1 < y < 1$ can be divided into intervals with step sizes $\Delta t = 0.0001$ and $\Delta y = 0.005$ for time and space respectively. Smaller step sizes do not show any significant change in the results. Convergence of the scheme is assumed when all of the unknowns u , w , A , B , θ and H for the last two approximations differ from unity by less than 10^{-6} for all values of y in $-1 < y < 1$ at every time step. Less than 7 approximations are required to satisfy this convergence criteria for all ranges of the parameters studied here.

3. RESULTS AND DISCUSSION

Figure 1 show the time development of the profiles of the velocity and temperature for $Ha = 1$, $m = 3$, $S = 0$, $a = 0.5$ and $b = 0.5$. The velocity and temperature distributions do not reach steady state monotonically as shown in figure. They increase with time up till a maximum value and then decrease up to the steady state under the effect of the decaying pressure gradient. The velocity component u reaches steady state faster than w which, in turn, reaches steady state faster than θ . This is expected as u is the source of w , while both u and w are sources of θ .

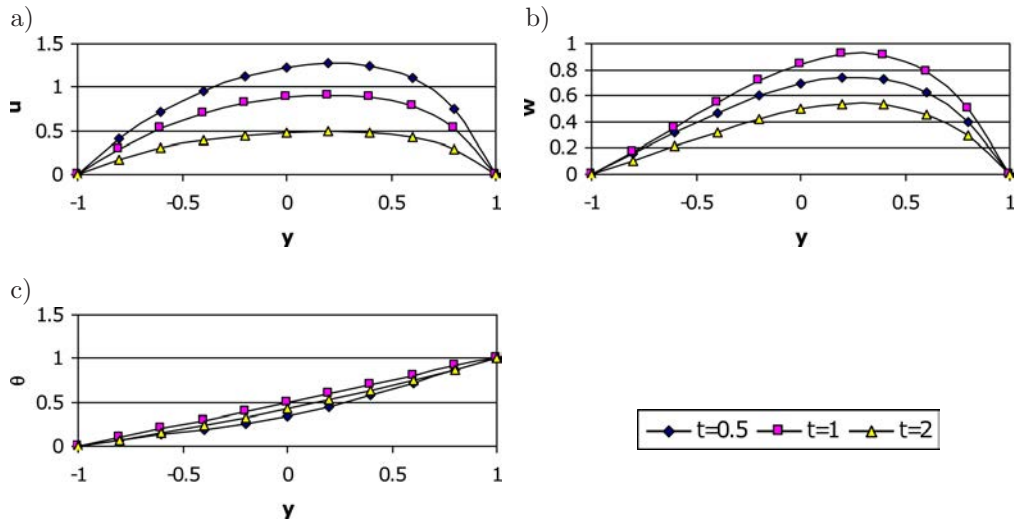


FIG. 1. The evolution of the profile of: a) u ; b) w ; c) θ ($Ha = 3$, $m = 3$, $S = 1$, $a = 0.5$, $b = 0.5$).

Figure 2 presents the time progression of the velocity component u at the centre of the channel ($y = 0$) for different values of m and a and for $b = 0$, $S = 0$ and $Ha = 3$. The figure indicates that u increases with m for all values of a which can be attributed to the fact that an increment in m decreases the effective conductivity ($\sigma/(1 + m^2)$) and then decreases the magnetic resistive force. The figure depicts also that the effect of a on u depends on the parameter m and becomes more clear for higher m .

Figure 3 shows the time progression of the velocity component w at the centre of the channel ($y = 0$) for different values of m and a and for $b = 0$, $S = 0$ and $Ha = 3$. The figure indicates that w increases with increasing m for all values of a as w is a result of the Hall effect. Although the Hall current is the source for w , Fig. 3 shows that, at small times, for large values of m , an increase in m produces a decrease in w . This can be understood by discussing the term

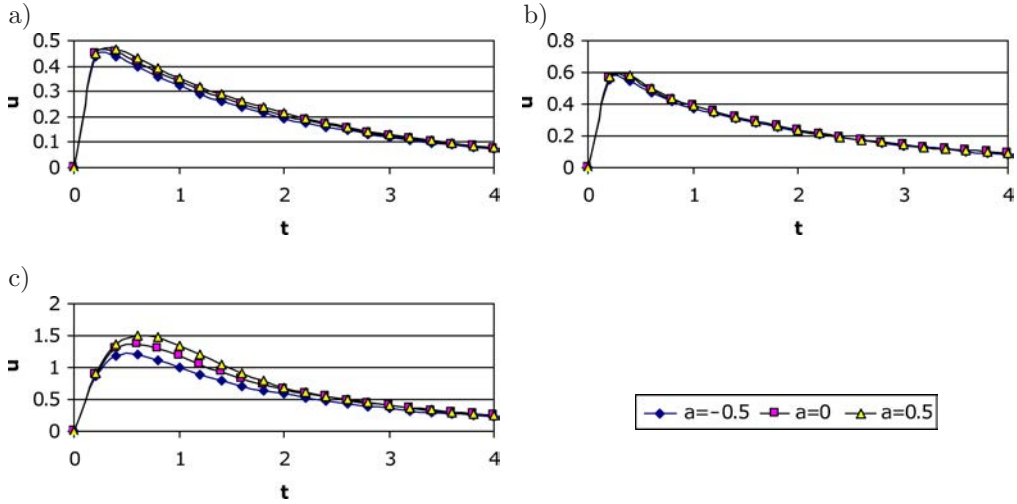


FIG. 2. The evolution of u at $y = 0$ for various values of a and m :
 a) $m = 0$; b) $m = 1$; c) $m = 5$ ($Ha = 3, S = 0, b = 0$).

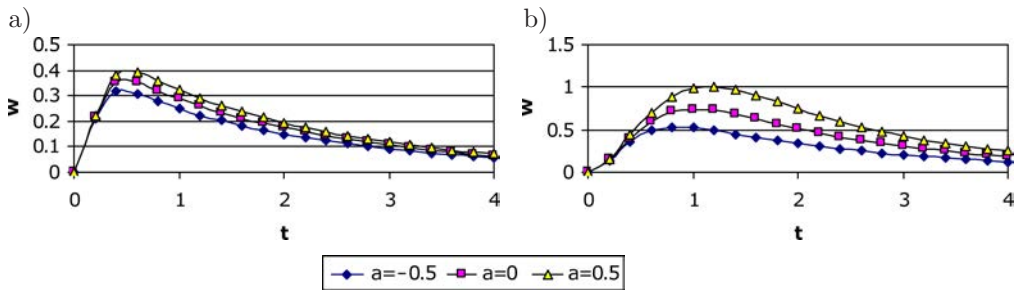


FIG. 3. The evolution of w at $y=0$ for various values of a and m :
 a) $m = 1$; b) $m = 5$ ($Ha = 3, S = 0, b = 0$).

$(-(w - mu)/(1 + m^2))$ in Eq. (2.10), which is the source term of w . At small times w is very small and this term may be approximated to $(mu/(1 + m^2))$, which decreases with increasing m if $m > 1$. Figure 3 presents also that the time required for w to reach its steady state value increases with increasing m and that w and its steady state time increase as a result of increasing a .

Figure 4 shows the time progression of the temperature θ at the centre of the channel for different values of m and a when $b = 0$ and $Ha = 3$. The variation of θ with m is shown to depend on t . When $m > 1$, increasing m decreases θ slightly at small times but increases θ at large times. This is because when t is small, u and w are small and an increment in m results in an increase in u but a decrease in w , so the Joule dissipation which is proportional also to $(1/(1 + m^2))$ decreases. When t is large, u and w increase with increasing m

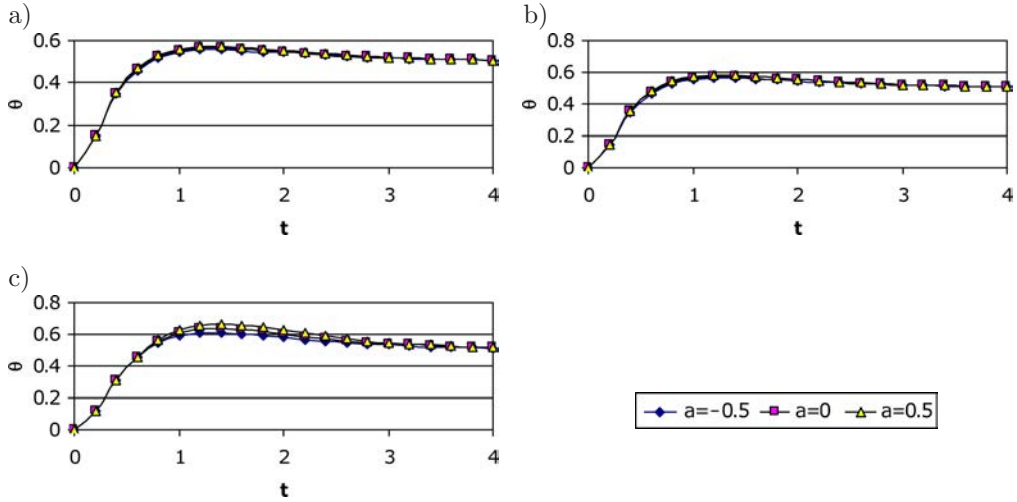


FIG. 4. The evolution of θ at $y = 0$ for various values of a and m :
 a) $m = 0$; b) $m = 1$; c) $m = 5$ ($Ha = 3, S = 0, b = 0$).

and so do the Joule and viscous dissipations. It is difficult to predict the effect of a on θ , because while increasing a increases the velocities and the velocity gradients, it decreases the function f_1 . All the same, Fig. 4 shows that increasing a increases θ and its effect is more apparent for higher values of m .

Figure 5 shows the time progression of θ at the centre of the channel for different values of m and b when $a = 0, S = 0$ and $Ha = 3$. The figure indicates that increasing b increases θ and its steady state time for all m . This occurs as

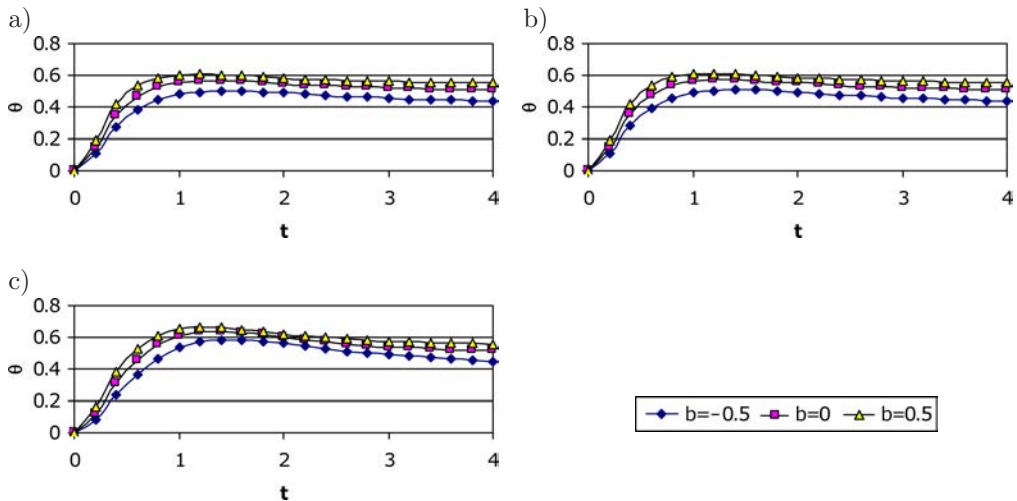


FIG. 5. The evolution of θ at $y = 0$ for various values of b and m :
 a) $m = 0$; b) $m = 1$; c) $m = 5$ ($Ha = 3, S = 0, a = 0$).

the centre of the channel acquires heat by conduction from the upper hot plate. The parameter b has no significant effect on u or w in spite of the coupling between the momentum and energy equations as depicted in figure.

Table 1 shows the dependence of the steady state temperature at the centre of the channel on a and m for $b = 0$ and $S = 0$. It is observed that θ increases with increasing m or a , as increasing m decreases damping forces and increasing a decreases viscosity. Both effects increase u , w and their gradients and hence the dissipations. Table 2 shows the variation of θ at the centre of the channel with m and b for $a = 0$, $S = 0$ and $Ha = 1$. The dependence of θ on m is explained by the same argument used in discussing Table 1. Table 2 indicates that increasing b increases θ since the centre acquires temperature by conduction from the upper hot plate. Table 3 presents the variation of θ with a and b for

Table 1. Variation of the steady state temperature θ at $y = 0$ for various values of m and a ($Ha = 1$, $b = 0$).

θ	$m = 0.0$	$m = 0.5$	$m = 1.0$	$m = 3.0$	$m = 5.0$
$a = -0.5$	0.5142	0.5144	0.5146	0.5152	0.5153
$a = -0.1$	0.5179	0.5183	0.5189	0.5201	0.5204
$A = 0.0$	0.5191	0.5195	0.5201	0.5271	0.5221
$A = 0.1$	0.5203	0.5207	0.5216	0.5235	0.5239
$A = 0.5$	0.5261	0.5269	0.5286	0.5333	0.5345

Table 2. Variation of the steady state temperature θ at $y = 0$ for various values of m and b ($Ha = 1$, $a = 0$).

θ	$m = 0.0$	$m = 0.5$	$m = 1.0$	$m = 3.0$	$m = 5.0$
$b = -0.5$	0.4562	0.4568	0.4579	0.4605	0.4611
$b = -0.1$	0.5077	0.5081	0.5089	0.5106	0.5109
$B = 0.0$	0.5191	0.5195	0.5201	0.5217	0.5221
$B = 0.1$	0.5295	0.5298	0.5304	0.5319	0.5322
$B = 0.5$	0.5609	0.5611	0.5616	0.5626	0.5628

Table 3. Variation of the steady state temperature θ at $y = 0$ for various values of a and b ($Ha = 1$, $m = 3$).

θ	$a = -0.5$	$a = -0.1$	$a = 0.0$	$a = 0.1$	$a = 0.5$
$b = -0.5$	0.4593	0.4579	0.4605	0.4634	0.4792
$b = -0.1$	0.5035	0.5089	0.5106	0.5125	0.5232
$B = 0.0$	0.5152	0.5201	0.5217	0.5235	0.5333
$B = 0.1$	0.5258	0.5304	0.5319	0.5335	0.5426
$B = 0.5$	0.5580	0.5615	0.5626	0.5639	0.5707

large and small values of Ha and for large and small values of m and for $Ha = 1$ and $m = 3$. Increasing a or b increases θ as explained above.

Figures 6, 7, and 8 show the time progression of the velocity components u and w and the temperature θ , respectively, at the centre of the channel ($y = 0$) for different values of S and a when $Ha = 3$, $m = 3$, and $b = 0$. Figures 6 and 7 show that increasing S decreases both u and w for all a due to the convection of the fluid from regions in the lower half to the centre which has higher fluid

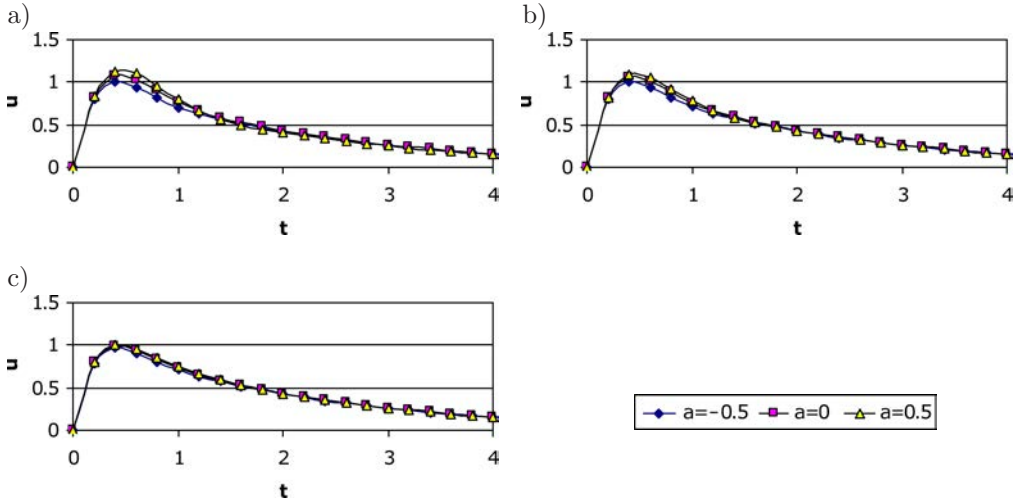


FIG. 6. The evolution of u at $y = 0$ for various values of a and S :
 a) $S = 0$; b) $S = 1$; c) $S = 2$ ($Ha = 3$, $m = 3$, $b = 0$).

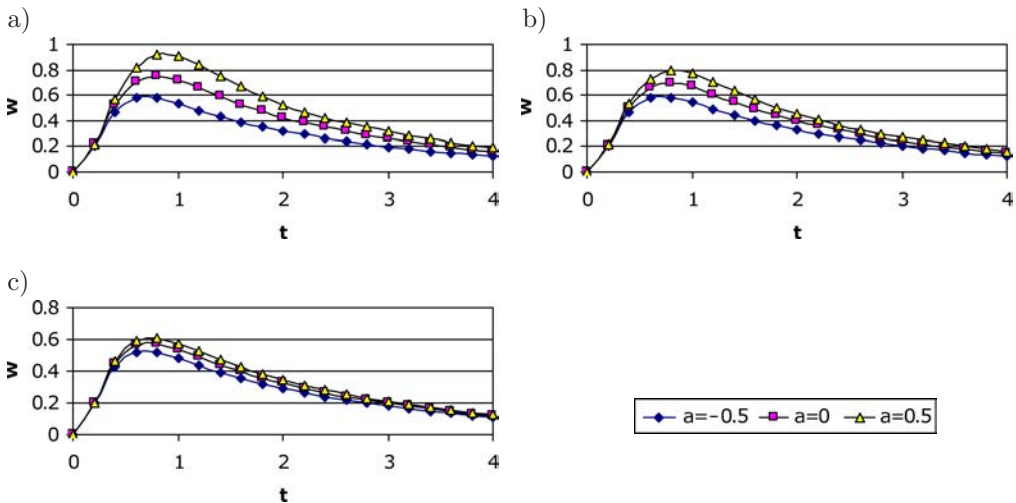


FIG. 7. The evolution of w at $y = 0$ for various values of a and S :
 a) $S = 0$; b) $S = 1$; c) $S = 2$ ($Ha = 3$, $m = 3$, $b = 0$).

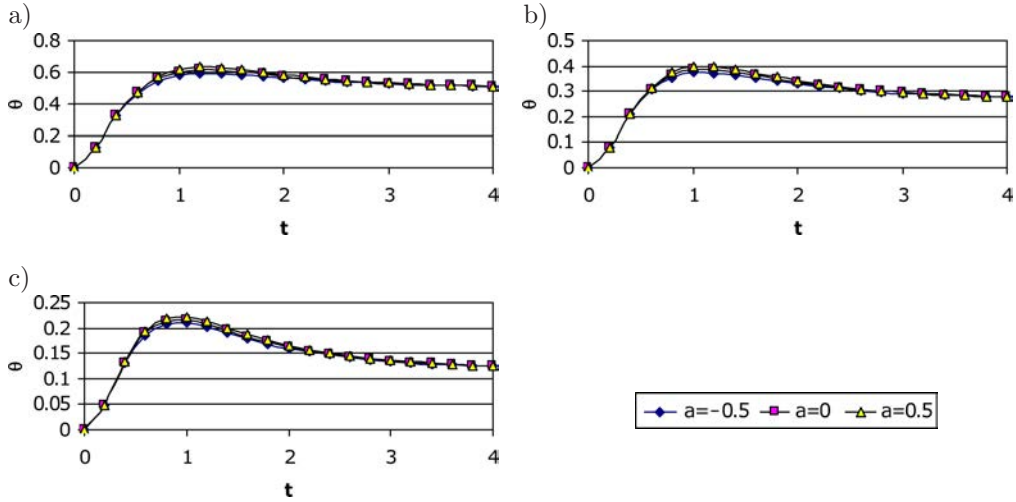


FIG. 8. The evolution of θ at $y = 0$ for various values of a and S :
 a) $S = 0$; b) $S = 1$; c) $S = 2$ ($Ha = 3, m = 3, b = 0$).

speed. It is also indicated that the influence of the parameter a on u and w becomes more apparent for lower values of the parameter S . Figure 8 indicates that increasing the suction parameter decreases the temperature θ for all a as a result of the influence of convection in pumping the fluid from the cold lower half towards the centre of the channel.

Figure 9 shows the evolution of the temperature θ at the centre of the channel ($y = 0$) for different values of S and b when $Ha = 3, m = 3$, and $a = 0$. The figure

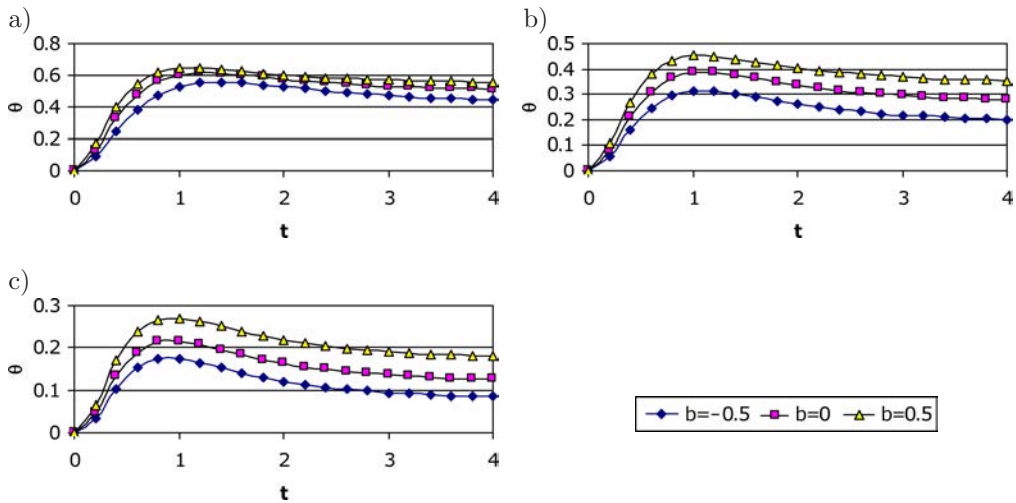


FIG. 9. The evolution of θ at $y = 0$ for various values of b and S :
 a) $S = 0$; b) $S = 1$; c) $S = 2$ ($Ha = 3, m = 3, a = 0$).

indicates that increasing S decreases θ for all b . Figure 9a shows that, for $S = 0$, the variation of θ with the parameter b depends on time as shown before in Fig. 5c for higher values of the Hall parameter m . Figures 9b and 9c present an interesting effect for the suction parameter in the suppression of the crossover points of the $\theta - t$ graph corresponding to various values of b . It is also seen that the effect of increasing the parameter b on θ is more pronounced for higher values of suction velocity.

4. CONCLUSIONS

The time varying MHD flow between two parallel plates was investigated considering the Hall current. The viscosity and thermal conductivity of the fluid are assumed to be temperature dependent. The effects of the Hartmann number Ha , the Hall parameter m , the viscosity variation parameter a and the thermal conductivity variation parameter b on the velocity and temperature fields at the centre of the channel are discussed. Introducing the Hall term gives rise to a velocity component w in the z -direction and affects the main velocity u in the x -direction. It is found that the parameter a has a marked effect on the velocity components u and w for all values of m . However, the parameter b has no significant effect on u or w . The results show that the effect of the parameter m on θ depends on t . For small time t , θ decreases with increasing m , but when t is large, or at steady state, θ increases with increasing m . The effect of the parameter m on the steady state time is ignored.

REFERENCES

1. HARTMANN J., LAZARUS F., *Kgl. Danske Videnskab. Selskab, Mat.-Fys. Medd.*, **15**, 6-7, 1937.
2. TAO L.N., *Magnetohydrodynamic effects on the formation of Couette flow*, *Journal of Aerospace Sci.*, **27**, 334, 1960.
3. ALPHER R.A., *Heat transfer in magnetohydrodynamic flow between parallel plates*, *International Journal of Heat and Mass Transfer*, **3**, 108, 1961.
4. SUTTON G.W., SHERMAN A., *Engineering Magnetohydrodynamics*, McGraw-Hill, 1965.
5. CRAMER K., PAI S., *Magnetofluid dynamics for engineers and applied physicists*, McGraw-Hill, 1973.
6. NIGAM S.D., SINGH S.N., *Heat transfer by laminar flow between parallel plates under the action of transverse magnetic field*, *Quart. J. Mech. Appl. Math.*, **13**, 85, 1960.
7. SOUNDALGEKAR V.M., VIGHNESAM N.V., TAKHAR H.S., *Hall and ion-slip effects in MHD Couette flow with heat transfer*, *IEEE Transactions on Plasma Sciences*, **PS-7**, 3, 1979.
8. SOUNDALGEKAR V.M., UPLEKAR A.G., *Hall effects in MHD Couette flow with heat transfer*, *IEEE Transactions on Plasma Science*, **PS-14**, 5, 1986.

9. ATTIA H.A., *Hall current effects on the velocity and temperature fields of an unsteady Hartmann flow*, Can. J. Phys., **76**, 739–746, 1998.
10. HERWIG H., WICKEN G., *The effect of variable properties on laminar boundary layer flow*, Wärme-und Stoffübertragung, **20**, 47–57, 1986.
11. KLEMP K., HERWIG H., SELMANN M., *Entrance flow in channel with temperature dependent viscosity including viscous dissipation effects*, Proceedings of the Third International Congress of Fluid Mechanics, Cairo, Egypt, **3**, 1257–1266, 1990.
12. ATTIA H.A., KOTB N.A., *MHD flow between two parallel plates with heat transfer*, Acta Mechanica, **117**, 215–220, 1996.
13. ATTIA H.A., *Transient MHD flow and heat transfer between two parallel plates with temperature dependent viscosity*, Mechanics Research Communications, **26**, 1, 115–121, 1999.
14. ZUECO J., EGUÍA P., GRANADA E., MÍGUEZ J.L., BEG O.A., *An electrical network for the numerical solution of transient MHD Couette flow of a dusty fluid: effects of variable properties and Hall current*, Int. Comm. Heat and Mass Trans., **37**, 10, 1432–1439, 2010.
15. EGUÍA P., ZUECO J., GRANADA E., PATIO D., *NSM solution for unsteady MHD Couette flow of a dusty conducting fluid with variable viscosity and electric conductivity*, Applied Mathematical Modelling, **35**, 303–316, 2011.
16. WHITE M.F., *Viscous fluid flow*, McGraw-Hill, 1991.
17. AMES W.F., *Numerical solutions of partial differential equations*, Second ED., Academic Press, New York, 1977.

Received September 12, 2011; revised version July 4, 2012.
